SEMARAK ILMU PUBLISHING

Journal of Advanced Research in Applied Sciences and Engineering Technology

Journal homepage:
https://semarakilmu.com.my/journals/index.php/applied_sciences_eng_tech/index
ISSN: 2462-1943

Lung Infection Detection via CT Images and Transfer Learning Techniques in Deep Learning

Marwa A. Shames[1], Mohammed Y. Kamil[1,*]

[1] College of Science, Mustansiriyah University, Baghdad ,Iraq

ARTICLE INFO

Article history:
Received 15 January 2024
Received in revised form 19 May 2024
Accepted 5 June 2024
Available online 20 June 2024

Keywords:
Deep learning; Covid; Transfer learning; Lung; Classification; Diagnosis

ABSTRACT

Healthcare systems are battling the global coronavirus epidemic with limited resources, requiring early diagnosis and enhanced tools for pandemic prevention. The computer can aid in diagnosis via computed tomography images like PCR. Deep learning and machine learning are popular methods, and their main contributions are COVID-19 detection and prediction. This work aimed to develop an AI-based early detection strategy for COVID-19 based on computed tomography images. The model was trained and tested using a dataset that includes CT images. The SARS-COV-2 dataset contains 2482 CT images of 210 patients from publicly available sources. The modified model demonstrated encouraging outcomes by greatly enhancing the sensitivity measure (95.82±1.75), which is an essential criterion for accurately detecting instances of COVID-19 infection. In addition, the model generated higher values for the accuracy metric (91.67±1.68), the specificity (88.08±3.72), the precision metric (87.51±3.27), the F1_score (91.43±1.55), and the area under the curve (91.98±1.55). Deep learning techniques significantly facilitate the early detection of COVID-19. Its use has the potential to improve clinical doctors' readiness and the management of pandemics.

1. Introduction

In recent years, there has been significant progress in the use of artificial intelligence (AI) methodologies, namely machine learning (ML) and deep learning (DL), within the field of medical imaging [1, 2]. AI systems have shown significant progress in the domain of image identification, which plays a crucial role in the diagnosis and detection of illnesses. Recent studies have shown that AI-assisted imaging systems have exhibited comparable diagnostic performance to that of human medical professionals in some medical conditions [3, 4]. SARS-CoV-2, an emerging coronavirus responsible for the onset of COVID-19 disease in human beings, first manifested in Wuhan, China, in December 2019 [5]. Individuals who get infected with COVID-19 may potentially have catastrophic consequences. Within a limited timeframe, several scientists have endeavored to develop a diverse array of screening equipment and classification methods. The reverse transcriptase-polymerase chain reaction (RT-PCR) is an essential screening approach for detecting severe acute respiratory

* *Corresponding author.*
E-mail address: m80y98@uomustansiriyah.edu.iq

https://doi.org/10.37934/araset.47.1.206218

syndrome (SARS) - COV-2 and COVID-19 [6]. Although RT-PCR is widely regarded as the primary method for first COVID-19 identification, it does possess several limitations. Researchers have used chest radiography imaging as a diagnostic tool to identify COVID-19.

Computed tomography (CT) and radiograph scans of the lungs are increasingly being seen as reliable methods for identifying COVID-19. Those infected with COVID-19 may exhibit consolidation, ground-glass opacification, bilateral involvement, and peripheral and diffuse distribution in their lungs. It has been shown that CT scans of the lungs may identify COVID-19 in patients in both the acute and convalescent phases of the disease [7-9]. As only those with severe or chronic lung injuries would have anomalies on their CT scans after recovery, it is impossible to determine how many people are impacted by the disease using this method alone [10]. CT scanners are widely available at many different hospitals. It provides findings quickly, often in under 15 minutes. CT expands diagnostic capabilities and is increasingly used for primary diagnostic reasons [11].

This project aims to create and use a dependable system for identifying and classification COVID-19, utilizing image processing and deep learning techniques to achieve a superior degree of accuracy in classification. Furthermore, the research aims to underscore the significance of ML and DL techniques in the context of addressing the COVID-19 pandemic; specifically, the focus is on elucidating the role of DL methodologies. The structure of the paper is as follows: Section 2 of this research encompasses a compilation of pertinent literature. While a comprehensive description of a convolutional neural network is provided, In Section 3, we further discuss the approach behind the DL framework. Section 4 provides a comprehensive overview of the dataset utilized in this study. It includes detailed information on the dataset. In Section 5, we illustrate the architecture of the training model. In Section 6, we report the findings and analysis, followed by the conclusions in Section 7.

2. Related work

Clinical imaging, such as CT scans, may now be used to diagnose COVID-19 gratitude to the development of DL and ML methods. This section provides a summary of current developments in the realm of COVID-19 detection systems that have included DL methods. JavadiMoghaddam *et al.,* [12] suggested a distinguishable architecture for DL, in which this model's pooling layer combines pooling with the SE-block layer. To improve COVID-19 diagnostic performance and convergence time, the suggested model employs batch normalization and mish function. The suggested approach was assessed using data from two public hospitals. Also, it was contrasted with several other widely used deep neural networks (DNN). The outcomes showed a recognition time of 0.069 milliseconds in test mode and an accuracy of 99.03% in the graphics processing unit (GPU). The suggested model also produces the network outcomes for real-time applications and classification metrics parameters. M. Yousefzadeh *et al.,* [13] presented a method using DL for detecting COVID-19 in chest CT scans and a radiologist helper. The framework includes a feature extractor that is based on EfficientNet B3, they used the mosmed data cohort, patients from MasihDaneshvari Hospital, and the CC-CCII cohort. These datasets comprise the non-COVID-19, COVID-19, non-pneumonia, common pneumonia, and normal classifications and a total of 7184 images from 5693 participants. AUC ratings of 0.997, 0.989, and 0.954 were obtained for the evaluation of the framework On the MDH cohort, on the CC-CCII test set, and the totality of the mos meddata cohort. The findings show that the framework performs better than the other models. Finally, various specialists assessed the framework's diagnosing skills as an aid. Ahamed *et al.,* [14] built a DL-based COVID-19 case identification algorithm that was trained using data from a database of chest CT scans. The suggested model used a DL architecture called ResNet50V2 which has been updated. Four class labels were included in which dataset was used for

training the model: confirmed COVID-19 cases, typically confirmed and controls viral and bacterial pneumonia cases. The dataset was gathered from a wide range of freely available resources. Before feeding the information into the suggested model, the aggregated dataset underwent preprocessing with a sharpening filter. Using chest X-ray images, this model achieved an accuracy of 96.452 for four clinical samples with COVID-19 bacterial pneumonia 98.954% for two instances of COVID-19 Viral Pneumonia, and 97.242% for three cases of COVID-19 Bacterial Pneumonia. Utilizing data from CT scans of the chest, the model was able to correct an overall accuracy of 99.012% of COVID-19 community-acquired Pneumonia cases across three classes, and 99.99% across two classes. Li *et al.,* [15] suggested a DL ensemble-based aided diagnostic system. The technique combines the stacked generalization ensemble learning with the VGG16 DL to produce a cascade classifier. The cascade classifier is built using data from several different subsets of the training set, each of which is used to collect outlier information on the generalization behavior of the data set as a whole. The method was experimentally tested to categorize patients with new coronavirus pneumonia, patients with common pneumonia, and healthy controls with a prediction accuracy of 93.57%, specificity of 93.93%, a sensitivity of 94.21%, a precision of 89.40%, F1_score of 91.74%. The findings demonstrate that the suggested strategy performs well for classification and may greatly enhance DNNs' performance prediction across several different categories. Alshazly *et al.,* [16] adopted cutting-edge deep network topologies and offered a transfer learning approach that utilizes carefully scaled input created for each deep architecture to attain optimal performance. conducted many different sets of investigations on the CT scan for SARS-CoV-2 and the. In the dataset including SARS-CoV-2, the best models had average values of 99.4% for accuracy, 99.6% for precision, 99.8% for sensitivity, and 99.6% for specificity, respectively. Their F1_scores also averaged 99.4%. The interpretability of the data was significantly enhanced by the use of visualization tools, which offered graphical representations of the reasons provided by the models for their predictions. The acquired features are shown in the form of well-separated clusters, each of which represents a CT scan of a COVID-19 patient or a non-COVID-19 case, respectively.

3. Methodology

3.1 CNN and VGG16

CNNs have emerged as the predominant focus of research in the field of ML algorithms for diagnosing medical abnormalities using image analysis [17]. It is important to note that a basic neural network cannot effectively learn intricate features, in contrast to the capabilities shown by DL architectures. CNNs have shown exceptional efficacy in several domains, including image classification, object identification, and medical image analysis [18]. The fundamental concept behind a CNN is its ability to extract localized characteristics from inputs at higher levels and propagate them to lower layers to generate more intricate features. The composition of a CNN includes convolutional, pooling, and fully connected (FC) layers. CNN's essential component is the convolution layer. This layer processes visual information to identify specific details. A series of filters separates high-level and low-level visual characteristics. Common components of filters include matrices and pixels of varying dimensions. The filters are applied to determine the form of the feature map, which is the final matrix created. The nonlinear layer comes after the convolution layer and is where the order is created. Referring to this layer as the "Relu layer" is convenient because it is where things become activated. The Relu activation function converts negative feature map values to zero. To keep the network's computations and parameters manageable, this layer must shrink the representation. This allows for the detection and elimination of network incompatibilities. Here, we want to maintain just the most important parameters and cut down on the number of entries in the following layer as much

as possible. This avoids memorizing and minimizes the computational cost for later layers. After the convolutional layer, we often use a pooling layer to reduce the dimension of the output. Max-pooling is the most typical kind of pooling. When sending data, it just sends the maximum value of each region [19]. A typical CNN architecture has several convolutional layers, then pooling layers that reduce the output's dimension even more, and finally mapping the feature maps to a fully connected layer for classification. After processing the data multiple times through the convolution layer, non-linear layer, and pooling layer, a single lengthy feature vector is obtained at the flattening stage. Additionally, it is linked to the ultimate classification model, also known as a fully connected model. The final layer is a fully connected one, representing the output layer, with the classification percentages serving the classification result as a single vector of probabilities, which are then passed to the SoftMax (multi-class) or sigmoid (binary class) classifier to select the class with the highest probability. During network building, we include additional layers, such as organization or optimization layers, to boost the network's performance and prevent overfitting. The leakage layer and the batch normalization layer are two of the most popular types of layers. Batch normalization enables independent training of each layer in the network. In addition, it normalizes the output of the preceding activation layer by removing the batch mean and dividing the batch standard deviation to increase the neural network's consistency. The neural network utilizes an effective regularization technique known as dropout. Specifically, Srivastava *et al.,* [20] advocated this technique. Dropout is implemented during training by keeping the neuron active with a probability of P or by setting it to 0 [21].

The Visual Geometry Group at the University of Oxford built the VGG16 model with the primary objective of achieving victory in the 2014 International Large-Scale Visual Recognition Challenge (ILSVRC2014) [22]. The Visual Geometry Group at the University of Oxford created the convolutional neural network architecture known as VGG16. A convolutional neural network consisting of 16 layers is similar to the architecture used in the VGG-16 model. The model starts with a set of weights acquired by training on the ImageNet dataset, which comprises more than 14 million images annotated with 1000 distinct categories. The VGG16 model has 138,357,544 parameters. Figure 1 shows the VGG16 model architecture.

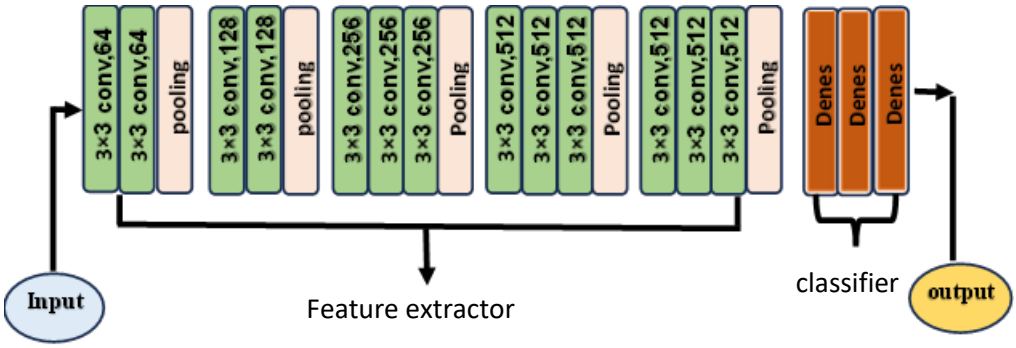

Fig. 1. VGG16 model architecture

3.2 Transfer Learning, Fine-Tuning, and Embedding

It seems that individuals possess inherent cognitive mechanisms that facilitate the assimilation of acquired knowledge into novel situations. In other words, when faced with unknown challenges, individuals possess the ability to leverage and use their prior knowledge and experiences. The capacity to establish connections between prior knowledge and new information is crucial for achieving success while acquiring new skills or knowledge. In contrast, a significant proportion of ML algorithms tend to focus on certain difficulties. Transfer learning (TL) enhances conventional ML

techniques by utilizing knowledge acquired from one or many source tasks to improve the learning process of a related target task [23]. The bulk of techniques for transferring work are essentially derived from the foundational ML algorithms used in task learning. Certain applications of TL use the principles of inductive learning. These applications include the modification and enhancement of established classification and inference techniques, such as neural networks, Bayesian networks, and Markov logic networks. The applications discussed in the literature use inductive learning techniques. Once CNN has learned to recognize one set of items, it needs to undergo retraining to recognize another set of objects that were not initially optimized for [24]. This research used a multi-step process, one of its components being fine-tuning in Keras. The first step in stopping backpropagation's reverse pass from reaching the network's head is to freeze all layers below it. The second step is to remove the network's endpoints and replace them with new, blank nodes. Learning via transfer lays the groundwork for the technique known as fine-tuning a network, which is an iterative process. We begin by training CNN to learn features for a large domain using a classification function that targets the creation of the least possible error in that domain. This training takes place using a broad domain as the training set. We then adjust the classification function and make other enhancements to the network to reduce errors in a new and more specialized domain. We are shifting the features and parameters of the network from the general domain into the more specific domain as part of this setup.

Conceptual modeling is often used for real-world problems to capture and integrate the specific needs of domain experts and technical specialists to facilitate the creation of information systems [25]. The integration of ML models into information systems to provide predictive functionality is becoming more common. Because complicated ML models are sometimes referred to as black boxes, it is an essential research topic to determine which methodologies and formalisms may be utilized to assess the correspondence between conceptual models and ML models. During training, the model accumulates convolutional layer kernels and fully connected layer weights. As a result, the discrepancies between performance predictions and ground truth labels on training datasets have decreased.

4. Dataset and Work Environment

The study utilized the Python programming language. The package utilizes Keras, a freely available and open-source Python framework for DL, which is fully compatible with TensorFlow. The software seamlessly integrates with the widely used NumPy and SciPy libraries for scientific and numerical computations in the Python programming language. Google's Colab notebooks were used for executing this implementation. After the acquisition of data, it is necessary to undergo a pre-processing stage to ensure that it adheres to the requirements of the model under development. The pre-processing stage, which is the first step in the use of images, presents key features of the images. In this discussion, we examine the enhancements made to the initial CT datasets. There are several possibilities. Pre-processing plays a crucial role in facilitating the learning process of the system and enabling the extraction of relevant image data. The methodology encompasses the use of data augmentation techniques, image normalization procedures, rescaling operations, and dataset partitioning. The inclusion of images from many data sets and cameras necessitates the resizing of their dimensions. The proposed study included resizing all images within both datasets to dimensions of 224 × 224. To improve the quality of CT images, it is essential to use image normalization as a crucial step in the suggested methodology. Pre-processing might potentially enhance the algorithm's ability to rapidly learn and extract features from images, thereby reducing the duration of the training process. This section comprehensively explains the formula used for normalization. The

consideration of X = x/255 is also necessary. The process of data augmentation. One often-used pre-processing technique is augmenting the dataset by introducing more instances and introducing noise into the images, providing the neural network with a greater amount of information. In this study, we introduce publicly accessible image datasets containing CT images. The dataset provided is public on the Kaggle website. SARS-COV-2 is a descriptive designation for the 2482 images they obtained for the initial dataset. The biggest image is 534x341, and the smallest is 244x145; they are all JPGs. To understand more about the classification's generalizability and its performance in retrospective studies employing patient demographic data, we will analyze DL representations in two sets. For both cases, we considered just axial CT volumes. Summarized below are the available datasets: SARS-CoV-2 CT scan dataset [26]. There are 210 patients represented on 2482 thoracic CT segments. Fifty people were negative for SARS-CoV-2 on CT (757 slices), whereas eighty tested positive (2,168 slices). The other 80 patients did not participate because they did not meet the criteria for the trial due to different lung problems. Using the radiologist's findings, we choose the best CT slice from each CT volume to feed into DL manually. The dataset was gathered from hospitals in Sao Paulo, Brazil, and patients' SARS-CoV-2 status was confirmed by RT-PCR testing. Figure 2 presents the block diagram for COVID-19 classification systems.

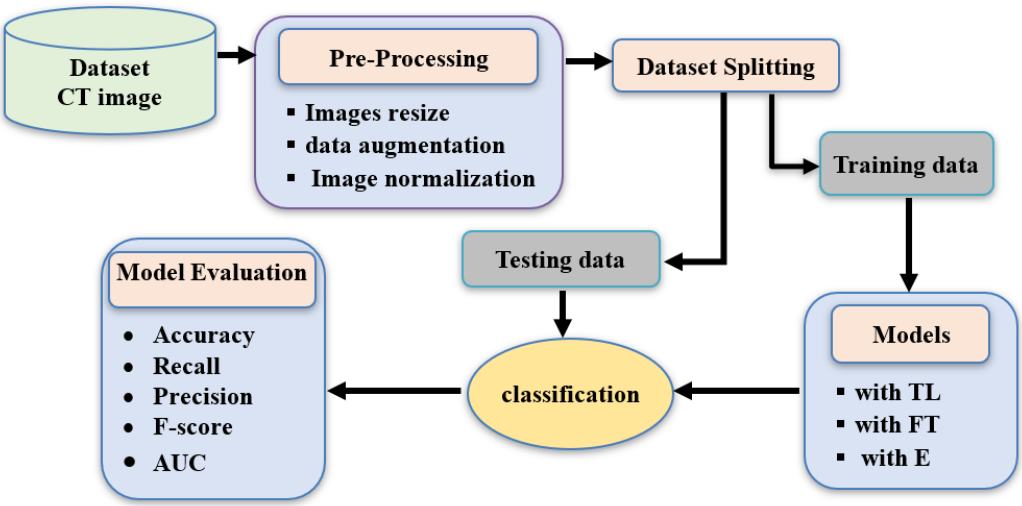

Fig. 2. Block diagram for COVID-19 classification systems

5. Architecture of Training Model

This research presents a unique combination method for the automated identification of COVID-19 patients. We used CNN and ML techniques in the design process of this building's architectural layout to produce the final product. In this particular investigation, CNN was used to extract automated qualities from the images. After recovering these characteristics, we send them to two additional classifiers: the Random Forest (RF) and the K-nearest neighbor (KNN). It is essential to recognize that the technique of hybrid models uses the same two datasets, in addition to similar pre-processing processes and a way of data division. The application will use the same convolutional neural network architecture described in the introduction. This will include the utilization of all layers, beginning with the first layer and ending with the sixth layer. The sole difference is that one uses the network simply for feature extraction, while the other uses it without the fully linked layers. TL, feature transformation (FT), and ML models, namely the KNN classifier, are non-parametric approaches in ML that are characterized by their efficiency, lack of assumptions, extensive adoption, and immediate responsiveness. Typically, the input vector of the KNN classifier comprises the feature

space and the target variable, which denotes the class membership. A majority voting procedure determines the class membership based on the classes of its neighboring instances. The majority vote determines the weights that represent the extent of separation between individual characteristic points and the centroid of the vector. and The RF classifier is a computational approach that offers predictive models for both classification and regression tasks. The ensemble models consist of several Decision Tree blocks that function as independent predictors. The underlying principle of this approach is to develop several predictors and aggregate their diverse forecasts, rather than attempt to achieve an optimum technique in a single iteration. The ultimate projected class is determined by selecting the class with the highest number of votes, which is the one that is used to carry out the classification process. Each of the three procedures will carry out the classification process on the same CT dataset. The approach proposed for implemented models is shown in Figure 3.

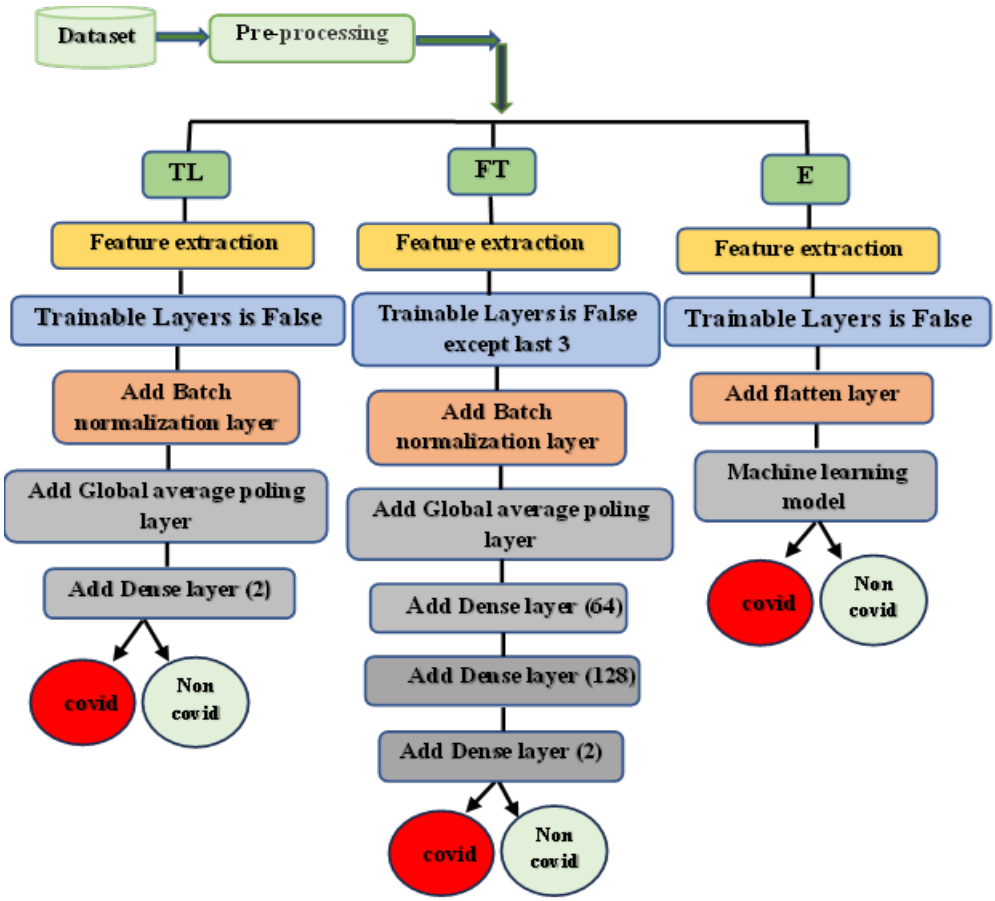

Fig. 3. The approach proposed for implemented models

6. Results and Discussion

We first split the dataset so that all classifiers had access to 80% for training and 20% for testing. Then, we revised the models by adding new trainable layers during training, and the fine-tuning of a neural network's parameters and hyperparameters is necessary. We included the learning rate, batch size, batch normalization, image resolution, and data augmentation approaches. Tuning parameters is an iterative process that needs multiple tries to attain a decent output. Finding the best values for a set of parameters is an optimization issue in and of itself. To identify hyperparameters that provide acceptable results, this procedure involves several iterations and trials. We trained every model using the Adaptive Moment Estimation (Adam) optimization method, starting with a learning rate of 0.001.

After 100 generations of evolution, we evaluate the constructed model on the test dataset to verify its validity. The batch size in the proposed system is 32. This decision is based on the empirical finding that smaller batch sizes often speed up the network training process while also using less memory. Consider the training accuracy, training loss, and validation loss per epoch to get a feel for the model's efficacy. The first iteration of the TL paradigm. The VGG16 model was used after including feature extraction and then setting trainable layers to false and including top to false. Subsequently, the model included three blocks, including the batch normalization layer, global average pooling 2D, and dense (2). Subsequently, include the classification of COVID-19 and non-COVID-19. The CNN model trained on the CT scan dataset is depicted in Figure 3, showcasing its accuracy. The figure displays the training accuracy, validation accuracy, loss retractions, and receiver operating characteristic (ROC) curve. The evaluation of CNN performance often employs performance indicators such as accuracy, sensitivity, specificity, precision, F1_score, and area under the curve (AUC). The performance indicators are shown. We determined the correctness of the model by evaluating the confusion matrix. The accuracy values obtained on the testing set were as follows: 79.07±0.92, 79.39±3.51, 78.80±2.73, 76.40±1.63, 77.81±1.30, and 79.08±0.99, as seen in Figure 4.

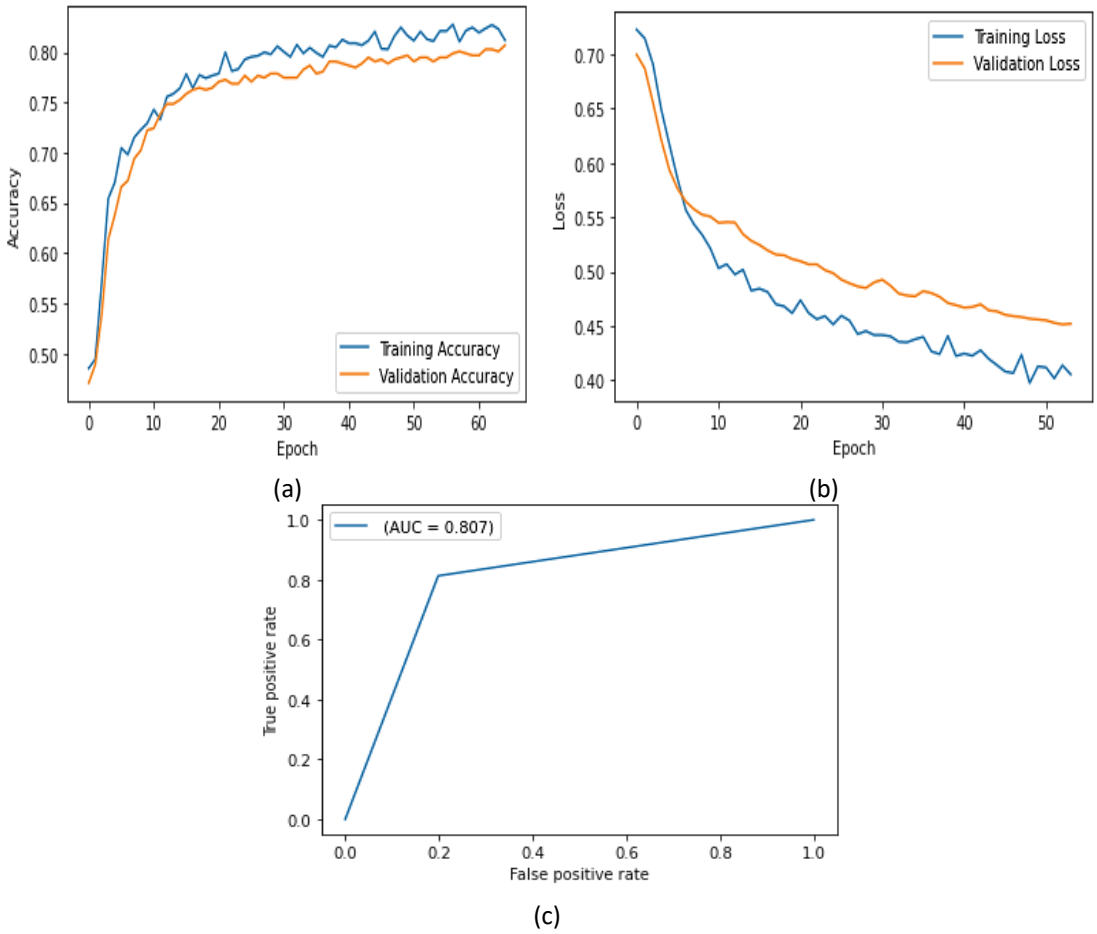

Fig. 4. TL model results using SARS-CoV-2: (a) accuracy, (b) loss, and (c) ROC curve

Due to the changes made to the second model, fine-tuning (FT), it is now possible to train only the three layers at the very bottom. After the inclusion of the three blocks of dense layer (64), dense layer (128), and dense layer (2), as well as the classifier, the model here implements the same TL model as in the previous section. COVID-19 has been After making certain changes to the parameters, we developed a new model with an overall accuracy that exceeded the TL model by 91.67±1.58

points. The final sensitivity, specificity, precision, F1_score, and AUC are higher than the TL model. These values are 95.82±1.75; 88.08±3.27; 87.51±3.27; 91.43±1.50; and 91.98±1.55, respectively. We trained the proposed CNN model on the CT scan dataset using FT. Figure 5 exhibits the training accuracy, validation accuracy, loss retractions, and ROC of the model.

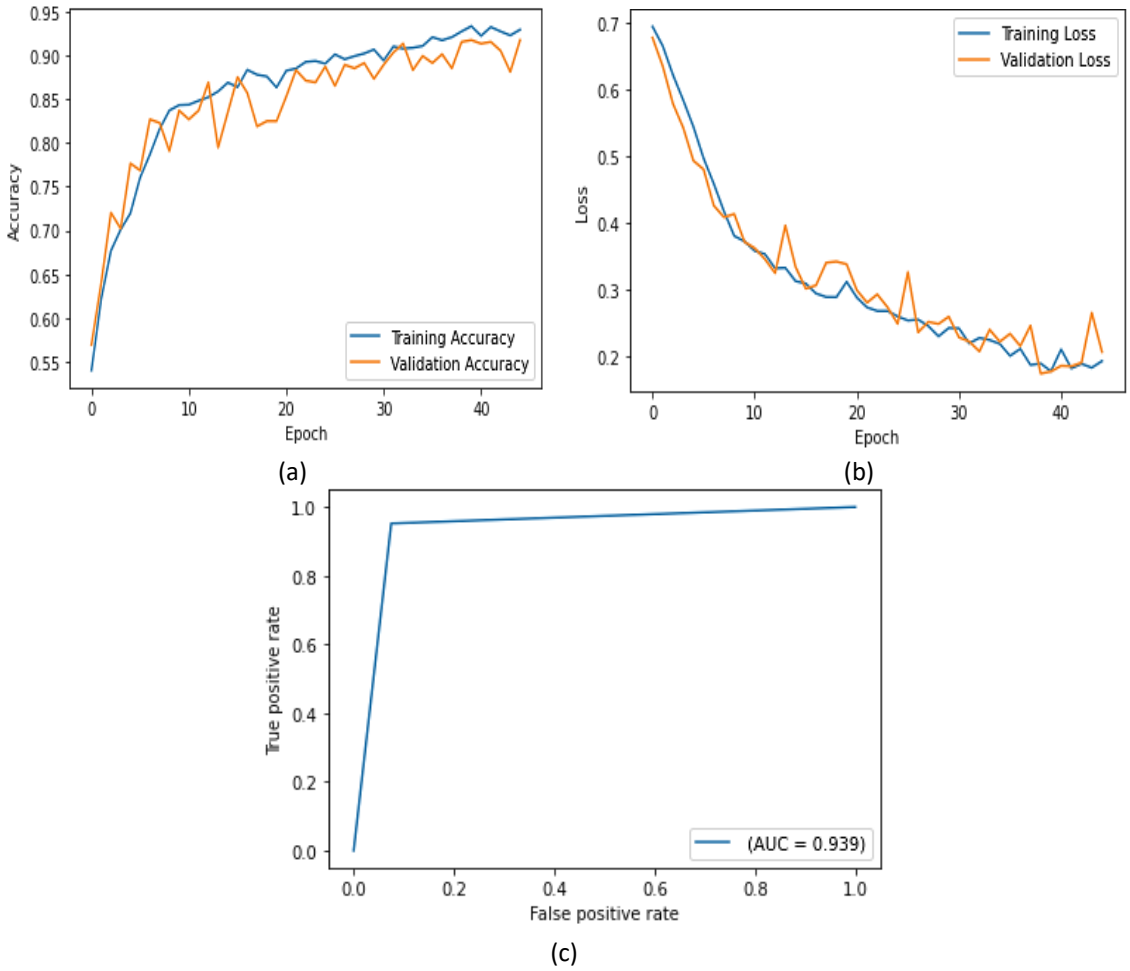

Fig. 5. FT model results using SARS-CoV-2: (a) accuracy, (b) loss, and (c) ROC curve

The third model uses the VGG16 model as a feature extractor. We built the model following the prescribed procedure: first, we set the trainable layer to false; then, we added a fake tope; next, we introduced a flattening layer; and finally, we appended the ML model sequentially. We initially utilized two distinct algorithms to instantiate the machine-learning model: the RF classifier and the KNN classifier. We initially utilized the RF classifier and then applied the KNN classifier in this research. The outcomes showed a somewhat reduced degree of efficacy in both situations as compared to the use of earlier methods. Combining DL with ML can achieve a more effective computational model, as demonstrated by this study. This enhanced efficiency, however, does not come without a cost, as seen by the results provided in Figure 6. The results show that the RF classifier achieved 52.51±3.15, 28.26±3.53, 71.16±3.61, 45.77±6.17, 34.94±4.32, and 50.7±3.13, respectively, for accuracy, sensitivity, specificity, precision, F1_score, and AUC. The mean accuracy for the KNN classifier ranged from 51.87±1.95 to 26±1.20, 74±3.66 to 46±3.64, and 33.34±1.51 to 50.08±1.84. The E method demonstrates that combining DL with ML results in faster model execution time. However, the combined accuracy is lower than that of the TL and FT models used separately.

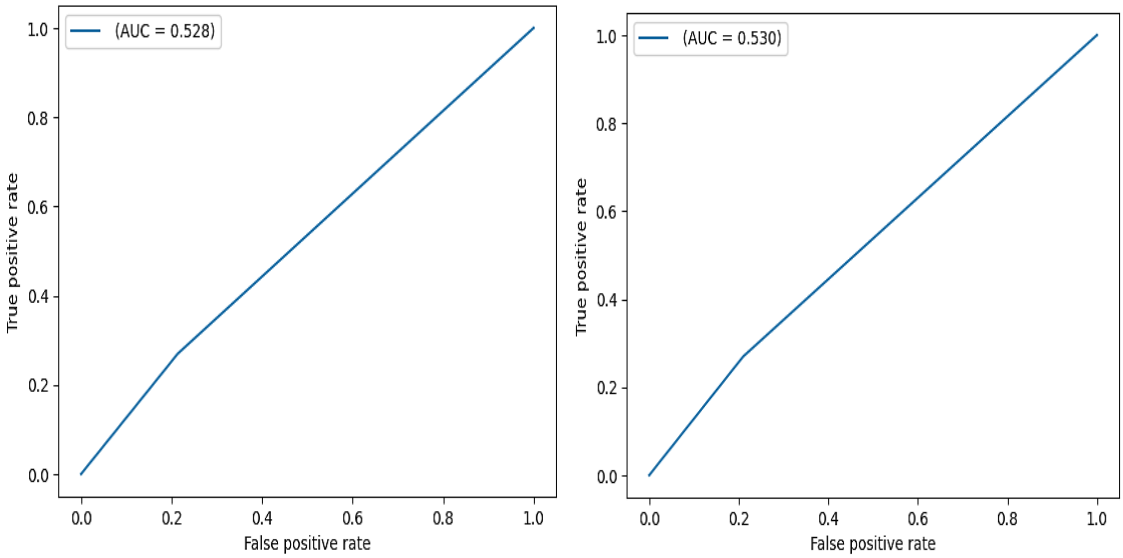

Fig. 6. Embedding model ROC curve using SARS-CoV-2: (a) RF (b) KNN

Accuracy, sensitivity, specificity, F1_score, precision, and AUC are only a few of the measures shown in Table 1. The findings demonstrated that the first approach, dubbed TL, had less-than-desirable results when compared to other approaches. When switching from the first method to the second, FT requires a somewhat different strategy. A subset of the TL approach known as FT was used in this instance. The unfreezing of the FT method's last three layers is what sets it apart from standard transfer-learning procedures and ultimately leads to the desired effect. This is why the last three layers, Denes Layers 64, Denes Layers 128, and Denes Layers 2, are given credit for improving the output quality by serving as extra classifiers for COVID and non-COVID situations. Generally, the strategy denoted by the letter E is considered the least efficient one. After creating a flattening layer, this method combines ML with DL by adding an ML model.

Table 1
Results for all methods

Method	Accuracy %	Sensitivity %	Specificity %	Precision %	F1_score %	AUC %
TL	79.07±0.92	79.39±3.51	78.80±2.73	76.40±1.63	77.81±1.30	79.08±0.99
FT	91.67±1.68	95.82±1.75	88.08±3.72	87.51±3.27	91.43±1.55	91.98±1.55
E_RF	52.51±3.15	28.26±3.53	71.16±3.61	45.77±6.17	34.94±4.32	50.7±3.13
E_KNN	51.87±1.95	26.00±1.20	74.15±3.62	46.61±3.64	33.34±1.51	50.08±1.84

In the last section, Table 2 presents a comprehensive summary of the results from several experiments done on the diagnostic system for COVID-19. The assessment was based on the correctness of the comparison. It is important to emphasize that direct comparisons are unfeasible owing to the discrepancies between the data sets, such as variations in the number of images and different methodologies used. However, when compared to earlier works, our study achieved superior results, reliability, and resilience for the FT model.

Table 2
Comparison with other works

References	Method	Accuracy %	Sensitivity %	Specificity %	Precision %	F1_score %	AUC %
[12]	WCNN4	99.03	98.91		98.71	98.43	
[13]	EfficientNB3		97.02	96.08		97.00	99.07
[14]	ResNet/class1	99.012	99.066	99.066	99.00		
	ResNet/class2	89.902	0.8991	90.15	89.706		
[15]	VGG16	93.57	94.21	93.93	89.40	91.74	
[16]	squeezeNet	95.1 ±1.3	96.2 ±1.4	94.0 ± 2.2	94.2 ± 2.0	95.2± 1.2	
	Shuffle Net	97.5 ± 0.8	99.0 ± 0.2	95.9 ± 1.5	96.1± 1.4	97.5± 0.8	
	ResNet18	98.3 ± 0.8	99.6 ± 0.3	97.1 ± 1.4	97.2± 1.2	98.4±.0.7	
	ResNet50	99.2± 0.3	99.4± 0.5	99.1 ± 0.5	99.1± 0.5	99.2±.0.3	
	ResNet101	99.4± 0.4	99.1 ± 0.6	99.6 ± 0.3	99.6 ± 0.3	99.4± 0.4	
	ResNeXt50	99.1± 0.5	99.3 ± 0.5	98.9 ± 0.6	99.0 ± 0.5	99.1±.0.5	
	ResNeXt101	99.2 ± 0.3	99.3± 0.5	99.2 ± 0.4	99.2 ± 0.4	99.2±0.3	
	InceptionV3	99.1± 0.5	99.8 ± 0.3	98.5 ± 0.8	98.5± 0.8	99.1±0.5	
	Xception	98.8± 0.6	98.6 ± 1.1	98.9 ± 1.1	99.0 ± 1.0	98.8±0.6	
	DenseNet11	99.3± 0.3	99.2 ± 0.5	99.4 ± 0.2	99.4± 0.2	99.3±0.3	
	DenseNet19	99.3± 0.5	99.3 ± 0.5	99.3 ± 0.7	99.4± 0.6	99.3±0.4	
	DenseNet201	99.2 ± 0.2	99.4 ± 0.2	98.9 ± 0.4	99.0± 0.4	99.2±0.2	
Our	TL	79.07±0.2	79.39±3.51	78.80±2.73	76.40±1.63	77.81±1.0	79.08±0.99
model	FT	91.67±1.8	95.82±1.75	88.08±3.72	87.51±3.27	91.43±1.5	91.98±1.55
	E_RF	52.51±3.5	28.26±3.53	71.16±3.61	45.77±6.17	34.94±4.2	50.70±3.13
	E_KNN	51.87±1.5	26.00±1.0	74.15±3.62	46.61±3.64	33.34±1.1	50.08±1.84

7. Conclusions

This study presents the development of a DL model, namely a VGG16 model, to diagnose COVID-19 based on chest CT scan images. We compared the redesigned model with other pre-existing models. The optimized model exhibited encouraging outcomes by significantly enhancing the sensitivity metric (95.82±1.75), a critical factor in the accurate detection of COVID-19 infection. Furthermore, the resulting model showed notable performance in terms of accuracy (91.67±1.68), specificity (88.08±3.72), precision (87.51±3.27), F1_score (91.43±1.55), and AUC (91.98±1.55). DL methodologies effectively identify and diagnose COVID-19 in chest CT scan images. DL has shown exceptional performance in the field of radiology. In future scenarios, the suggested methodology has the potential for clinical practitioners to use it as a means of analyzing, identifying, and subsequently preventing and managing pandemics more effectively.

Acknowledgment
The authors would like to thank Mustansiriyah University for their valuable support and for providing essential facilities for this research.

References
[1] Clement, J. Christopher, VijayaKumar Ponnusamy, K. C. Sriharipriya, and R. Nandakumar. "A survey on mathematical, machine learning and deep learning models for COVID-19 transmission and diagnosis." *IEEE reviews in biomedical engineering* 15 (2021): 325-340. https://doi.org/10.1109/RBME.2021.3069213

[2] Radhi, Eman A., and Mohammed Y. Kamil. "Breast Tumor Detection Via Active Contour Technique." *International Journal of Intelligent Engineering & Systems* 14, no. 4 (2021). https://doi.org/10.22266/ijies2021.0831.49

[3] Kadhim, Rania R., and Mohammed Y. Kamil. "Comparison of machine learning models for breast cancer diagnosis." *IAES International Journal of Artificial Intelligence* 12, no. 1 (2023): 415. https://doi.org/10.11591/ijai.v12.i1.pp415-421

[4] Kamil, Mohammed Y. "Morphological gradient in brain magnetic resonance imaging based on intuitionistic fuzzy approach." In *2016 Al-Sadeq International Conference on Multidisciplinary in IT and Communication Science and Applications (AIC-MITCSA)*, pp. 1-3. IEEE, 2016. https://doi.org/10.1109/AIC-MITCSA.2016.7759924

[5] De Sousa, Orrana LV, Deborah MV Magalhães, Pablo de A. Vieira, and Romuere Silva. "Deep learning in image analysis for COVID-19 diagnosis: a survey." *IEEE Latin America Transactions* 19, no. 6 (2021): 925-936. https://doi.org/10.1109/TLA.2021.9451237

[6] Bhowal, Pratik, Subhankar Sen, Jin Hee Yoon, Zong Woo Geem, and Ram Sarkar. "Choquet integral and coalition game-based ensemble of deep learning models for COVID-19 screening from chest X-ray images." *IEEE Journal of Biomedical and Health Informatics* 25, no. 12 (2021): 4328-4339. https://doi.org/10.1109/JBHI.2021.3111415

[7] Ruano, Josué, John Arcila, David Romo-Bucheli, Carlos Vargas, Jefferson Rodríguez, Óscar Mendoza, Miguel Plazas et al. "Deep learning representations to support COVID-19 diagnosis on CT slices." *Biomédica* 42, no. 1 (2022): 170-183. https://doi.org/10.7705/biomedica.5927

[8] Radhi, Eman, and Mohammed Kamil. "An automatic segmentation of breast ultrasound images using U-Net model." *Serbian Journal of Electrical Engineering* 20, no. 2 (2023): 191-203. https://doi.org/10.2298/SJEE2302191R

[9] Jangam, Ebenezer, Aaron Antonio Dias Barreto, and Chandra Sekhara Rao Annavarapu. "Automatic detection of COVID-19 from chest CT scan and chest X-Rays images using deep learning, transfer learning and stacking." *Applied Intelligence* (2022): 1-17. https://doi.org/10.1007/s10489-021-02393-4

[10] Kamil, Mohammed Y., and Sahar A. Hashem. "Segmentation of chest X-ray images using U-Net model." In *Mendel*, vol. 28, no. 2, pp. 49-53. 2022. https://doi.org/10.13164/mendel.2022.2.049

[11] Rana, Ashish, Harpreet Singh, Ravimohan Mavuduru, Smita Pattanaik, and Prashant Singh Rana. "Quantifying prognosis severity of COVID-19 patients from deep learning based analysis of CT chest images." *Multimedia Tools and Applications* 81, no. 13 (2022): 18129-18153. https://doi.org/10.1007/s11042-022-12214-6

[12] JavadiMoghaddam, SeyyedMohammad, and Hossain Gholamalinejad. "A novel deep learning based method for COVID-19 detection from CT image." *Biomedical signal processing and control* 70 (2021): 102987. https://doi.org/10.1016/j.bspc.2021.102987

[13] Yousefzadeh, Mehdi, Parsa Esfahanian, Seyed Mohammad Sadegh Movahed, Saeid Gorgin, Dara Rahmati, Atefeh Abedini, Seyed Alireza Nadji et al. "ai-corona: Radiologist-assistant deep learning framework for COVID-19 diagnosis in chest CT scans." *PloS one* 16, no. 5 (2021): e0250952. https://doi.org/10.1371/journal.pone.0250952

[14] Ahamed, Khabir Uddin, Manowarul Islam, Ashraf Uddin, Arnisha Akhter, Bikash Kumar Paul, Mohammad Abu Yousuf, Shahadat Uddin, Julian MW Quinn, and Mohammad Ali Moni. "A deep learning approach using effective preprocessing techniques to detect COVID-19 from chest CT-scan and X-ray images." *Computers in biology and medicine* 139 (2021): 105014. https://doi.org/10.1016/j.compbiomed.2021.105014

[15] Li, Xiaoshuo, Wenjun Tan, Pan Liu, Qinghua Zhou, and Jinzhu Yang. "Classification of COVID-19 chest CT images based on ensemble deep learning." *Journal of healthcare engineering* 2021 (2021). https://doi.org/10.1155/2021/5528441

[16] Alshazly, Hammam, Christoph Linse, Erhardt Barth, and Thomas Martinetz. "Explainable COVID-19 detection using chest CT scans and deep learning." *Sensors (Switzerland)* 21, no. 2 (2021): 1-22. https://doi.org/10.3390/s21020455

[17] Oyelade, Olaide Nathaniel, Absalom El-Shamir Ezugwu, and Haruna Chiroma. "CovFrameNet: An enhanced deep learning framework for COVID-19 detection." *Ieee Access* 9 (2021): 77905-77919. https://doi.org/10.1109/ACCESS.2021.3083516

[18] Acar, Erdi, Engin Şahin, and İhsan Yılmaz. "Improving effectiveness of different deep learning-based models for detecting COVID-19 from computed tomography (CT) images." *Neural Computing and Applications* 33, no. 24 (2021): 17589-17609. https://doi.org/10.1007/s00521-021-06344-5

[19] Masud, Mohd Akmal, Mohd Zamani Ngali, Siti Amira Othman, Ishkrizat Taib, Kahar Osman, Salihatun Md Salleh, Ahmad Zahran Md Khudzari, and Nor Salita Ali. "Variation Segmentation Layer in Deep Learning Network for SPECT Images Lesion Segmentation." *Journal of Advanced Research in Applied Sciences and Engineering Technology* 36, no. 1 (2023): 83-92. https://doi.org/10.37934/araset.36.1.8392

[20] Srivastava, Nitish, Geoffrey Hinton, Alex Krizhevsky, Ilya Sutskever, and Ruslan Salakhutdinov. "Dropout: a simple way to prevent neural networks from overfitting." *The journal of machine learning research* 15, no. 1 (2014): 1929-1958.

[21] Sakib, Sadman, Tahrat Tazrin, Mostafa M. Fouda, Zubair Md Fadlullah, and Mohsen Guizani. "DL-CRC: deep learning-based chest radiograph classification for COVID-19 detection: a novel approach." *Ieee Access* 8 (2020): 171575-171589. https://doi.org/10.1109/ACCESS.2020.3025010

[22] Russakovsky, Olga, Jia Deng, Hao Su, Jonathan Krause, Sanjeev Satheesh, Sean Ma, Zhiheng Huang et al. "Imagenet large scale visual recognition challenge." *International journal of computer vision* 115 (2015): 211-252. https://doi.org/10.1007/s11263-015-0816-y

[23] Das, N. Narayan, Naresh Kumar, Manjit Kaur, Vijay Kumar, and Dilbag Singh. "Automated deep transfer learning-based approach for detection of COVID-19 infection in chest X-rays." *Irbm* 43, no. 2 (2022): 114-119. https://doi.org/10.1016/j.irbm.2020.07.001

[24] Weiss, Karl, Taghi M. Khoshgoftaar, and DingDing Wang. "A survey of transfer learning." *Journal of Big data* 3 (2016): 1-40. https://doi.org/10.1186/s40537-016-0043-6

[25] Kamil, Mohammed Y., and Abdul-Lateef A. Jassam. "Analysis of tissue abnormality in mammography images using gray level co-occurrence matrix method." In *Journal of Physics: Conference Series*, vol. 1530, no. 1, p. 012101. IOP Publishing, 2020. https://doi.org/10.1088/1742-6596/1530/1/012101

[26] Soares, Eduardo, Plamen Angelov, Sarah Biaso, Michele Higa Froes, and Daniel Kanda Abe. "SARS-CoV-2 CT-scan dataset: A large dataset of real patients CT scans for SARS-CoV-2 identification." *MedRxiv* (2020): 2020-04. https://doi.org/10.1101/2020.04.24.20078584